Comparison of 2D and 3D finite element models of tunnelling in granular soil under existing raft foundation

Sumi Siddiqua & Ahmed ElMouchi
Department of Civil Engineering – University of British Columbia, Kelowna, British Columbia, Canada
Asmaa M. Hassan & Mohamed I. Amer
Department of Public Works – Faculty of Engineering - Cairo University, Jizah, Egypt

ABSTRACT
Modeling the excavation process of underground tunnels under existing raft foundations is a 3D problem. However, 2D plane strain analysis is used to study tunnel-raft performance especially during the preliminary design stage of a project. This study focuses on comparing 2D and 3D finite element modelling results. The TBM tunnelling process is modeled in 2D and 3D and the calculated ground surface settlement troughs have been validated with field measurements from a selected case study (Second Heinenoord Tunnel in the Netherlands). In the current study, the contraction ratio (C) is used to account for 3D effects in the 2D analysis. In addition, an extensive 3D sensitivity analysis is conducted to evaluate the effect of related parameters including; tunnel diameter (D), tunnel cover (Z), and horizontal clearance between the raft centerline and the tunnel centerline (CL). The results of the sensitivity analysis are used to obtain values for the contraction ratio (C) that account for the 3D behavior of the tunnelling process in granular soils.

RÉSUMÉ
La modélisation du processus d'excavation des tunnels souterrains sous la base de radeau existante est un problème 3D. Cependant, la 2D analyse de contrainte d'avion est employée pour étudier la représentation de tunnel-radeau particulièrement pendant l'étape de conception préliminaire d'un projet. Cette étude se concentre sur comparer entre le 2D et les modèles d'élément 3D fini. Le processus de perçage d'un tunnel de TBM est simulé utilisant 3D et le 2D élément fini et les cuvettes extérieures moulues calculées de règlement ont été validés avec des mesures sur le terrain d'une étude de cas sélectionnée (en second lieu tunnel de Heinenoord aux Pays-Bas). Dans l'étude actuelle, le rapport de contraction (c) est employé pour expliquer l'effet 3D en la 2D analyse. En outre, une étude paramétrique étendue est entreprise pour évaluer l'effet des paramètres relatifs comprenant ; percez un tunnel le diamètre (d), la couverture de tunnel (z), et le dégagement horizontal entre la ligne centrale de radeau et la ligne centrale de tunnel (CL). Les résultats de l'étude paramétrique sont employés pour obtenir les valeurs pour le rapport de contraction (c) qui expliquent le comportement 3D du processus de perçage d'un tunnel dans sols granulaires.

1 INTRODUCTION

Traffic congestion in urban areas causes a lot of social, health, environmental and economic problems. Hence, there is a need to construct underground transportation systems, such as underground Metro lines, in many residential areas to decrease the amount of vehicles and road users.

Constructing underground tunnels in residential areas is a major challenge particularly when the tunnel passes underneath an existing building. This is because the building is expected to suffer additional settlements and straining actions which might cause a functional or structural failure of the building (Maleki et al. 2011; Mroueh and Shahrour 2003).

The effect of tunnel construction on the existing building is considered a 3D problem. However, in preliminary design stages, a simplified 2D model might be adopted. In engineering practice, using 3D modelling, is a time consuming matter. Therefore, the tunnel is divided into several sections across its longitudinal profile. Then, the tunnel effect on each building is evaluated using simple 2D modelling technique which adopt plan strain assumptions. However, 2D plane strain analyses do not account for the arching effect or the volume loss around the face of the tunnel. The 3D arching effect around the tunnel means that the principal stresses around the tunnel are rotated and this rotation decreases the ground loads acting on the tunnel lining. The volume loss is defined as the ratio between the total volume of the surface settlement trough and the tunnel excavation volume (Vermeer and Brinkgreve 1993). The volume loss when constructing a shielded TBM tunnels can be attributed to two main reasons: (i) axial movement due to the ground movement towards the tunnel face as a reason for the stress relief and, (ii) radial movement due to the lining-shield gap and the lining deformation. In 2D analyses, the 3D arching effect and the volume loss are considered using either a pressure approach or a displacement approach (Moller 2006). The pressure approach reduces the initial ground pressure inside the tunnel down to the support pressure (Wood 1975). The displacement approach applies a prescribed contraction to the tunnel lining. In this research, the displacement approach is adopted.

In previous studies, the effect of the tunnel construction on an existing building was addressed by using either a coupled analysis or uncoupled analysis. The coupled analysis simulates both the tunnel and the building in the same model. In contrast, an uncoupled analysis calculates the greenfield surface settlement trough using empirical

equations (Peck 1969; O'Reilly and New 1982; Sugiyama et al. 1999). Afterwards, the resulting settlements are applied to the building and the building response is examined. In doing so, the uncoupled analysis neglects the 3D nature of the tunnel-building interaction and the building stiffness. To consider the building stiffness in the analysis, Addenbrooke and Potts (1997) presented an extensive parametric study using a 2D plane strain Finite Element (FE) analysis. They presented some modification factors to relate the deflection ratio and the horizontal strain of the building for wide range of stiffnesses and geometries to the corresponding greenfield situation. Franzius (2003) revisited the design approach proposed by Addenbrooke et al. (1997) and extended its applicability by verifying the field data obtained during the construction of Jubilee Line Extension in London (1979). Morevover, an extensive parametric study was carried out using both 2D and 3D FE analyses. This parametric study aimed to study the effect of the following parameters on the behavior of an existing building: The effect of the building geometry with respect to the tunnel direction, the effect of the nature of contact between the soil and the building foundation and the effect of the building weight. The results of this study helped in better understanding of the tunnel-building-soil interaction problem. In addition, Franzius (2003) verified and extended the applicability of the relative stiffness approach and added a greater confidence in this design approach in the engineering practice.

This paper presents a comparison between 2D and 3D FE models (using the PLAXIS © software) for the effect of tunnel construction on an existing building resting on a raft foundation. In this study, the coupled analysis procedure is adopted to account for the building stiffness during the tunnel construction. The paper consists of four parts. In the first part, the 2D and 3D numerical models of the tunnelling process are verified by comparing the greenfield surface settlement troughs resulting from the FE models with the measured green field surface settlement trough in field for a selected case study (the Second Heinenoord Tunnel in the Netherlands). The second part shows the proposed raft configuration and the stages of construction in both 2D and 3D analyses. The third part presents the results of the sensitivity analysis conducted in 3D to check the effect of related parameters including the soil relative density (D_r), the tunnel diameter (D), the tunnel cover (Z), and the horizontal clearance between the tunnel centerline and the raft centerline (CL). The last part illustrates the values of the contraction ratio (C) that are used in 2D analysis to account for the 3D arching and the volume loss around the tunnel.

2 CASE STUDY AND NUMERICAL MODEL VERIFICATION

The selected case study is the Second Heinenoord Tunnel which was constructed between 1996 and 1998 to connect the North and South banks of Oude Mass river in the Netherlands. The main reason for selecting this tunnel is the availability of field measurement data for the surface settlement trough which enabled Moller (2006) to simulate the tunnelling process using 2D and 3D FE models (PLAIXS ©) to compare the results of the numerical simulation with the field measurement.

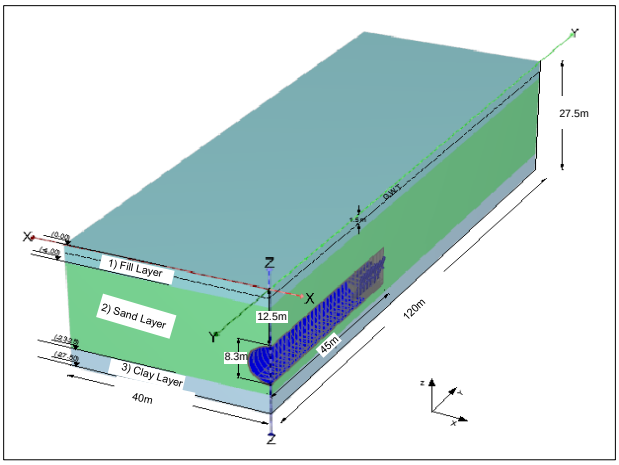

Figure 1. 3D model configuration of Second Heinenoord Tunnel after Moller (2006)

Figure 1 shows the 3D FE model for the Second Heinenoord Tunnel after Moller (2006). Due to symmetry, only half of the tunnel is simulated. At the monitored section of the Second Heinenoord tunnel, there were three different soil layers. The soil mass is simulated as a continuum of volume elements. For the 3D FE mesh, 10-node tetrahedrons are used. The Hardening Soil Model (HSM) is assigned for the three soil layers as stated in Table 1. The soil cover from the ground surface till to the tunnel crown equals 12.5 m and the tunnel outer diameter is 8.3 m. The ground water table is monitored at 1.5 m depth below the ground surface.

The Second Heinenoord tunnel is executed using a slurry shield Tunnel Boring Machine (TBM). The numerical simulation of the tunnelling process using 3D analysis comprises the following five components: (i) The tunnel lining: is simulated using shell element to represent the linear elastic concrete material, with a flexural rigidity EI = 26.78 MN.m^2, normal stiffness EA = 10.5 x 103 MN, weight w = 24 kN/m^2, and Poisson's ratio υ = 0.15, (ii) the TBM shield: is modeled as a radial pressure (125 kPa) and this value increases linearly with depth by 15 kPa/m, (iii) the slurry pressure at the face of the tunnel: has been accounted for by an axial pressure (230 kPa) that increases linearly with depth by 15 kPa/m, (iv) the tail grouting behind the shield: is simulated as a radial pressure (125 kPa) and this value increases linearly with depth by 15 kPa/m and (v) the ground-lining gap: is accounted for by deactivating a 20 cm thickness of soil volume elements at the tail of the shield and in the subsequent construction phases this gap is filled by a hardening grouting material which has the same lining material properties. The TBM length is 7.5 m and the tail grouting is 3.0 m long. The tunnel construction stages are divided into 30 slices. The length of each slice is 1.5 m, thus the total tunnel length is

45 m. This length has been chosen to ensure the steady-state condition for the surface settlement trough.

Table 1. Characteristics of soil layers used in the FE models for the Second Heinenoord Tunnel

Layer	(1) Fill	(2) Sand	(3) Clay
Layer Depth	0 – 4	4 – 23.5	23.5 – 27.5
Saturated unit weight, γ (kN/m^3)	17.2	20	20
Tangent stiffness for primary oedometer loading, E^{ref}_{oed} (MPa)	14	35	7
Secant stiffness in standard drained triaxial test, E^{ref}_{50} (MPa)	14	35	12
Unloading/Reloading stiffness, E^{ref}_{ur} (MPa)	42	105	35
Power for stress-level dependency of stiffness, m	0.5	0.5	0.9
Effective angle of shearing resistance, φ (deg.)	27	35	31
Effective cohesion, c' (kPa)	3	0.01	7
At rest Earth pressure coefficient, K_o	0.58	0.47	0.55
Poisson's ratio, υ_{ur}	0.2	0.2	0.2

The resulting surface settlement trough in this study is compared with the field measurement data and the surface settlement trough obtained from Moller's (2006) modelling as shown in Fig. 2. A good agreement between the three curves of the settlement trough is noted. The three greenfield settlement troughs show the same maximum settlement at the tunnel centerline (25 mm) and the same trough width (40 m). However, both settlement trough curves resulting from this study and Moller's (2006) model are flatter than the measured values. This could be attributed to the used Hardening Soil Model (HSM) for the different soil layers as explained by Moller (2006).

Figure 3 presents the 2D model for the Second Heinenoord Tunnel after Moller (2006). The displacement method is used to account for the 3D arching effect and the tunnel volume loss. According to Fig. 3, the same model geometry and soil profile that has been used in the 3D analysis, are used for the 2D analysis. The tunnel final lining has been simulated as a linear elastic concrete material, using shell element of the same properties of the tunnel lining in the 3D model. The tunnel final lining is surrounded by a rigid interface. Using 2D modelling, the settlement trough that best represents the field data was attained at a contraction ratio (C) equal to 0.7 as shown in Fig. 4.

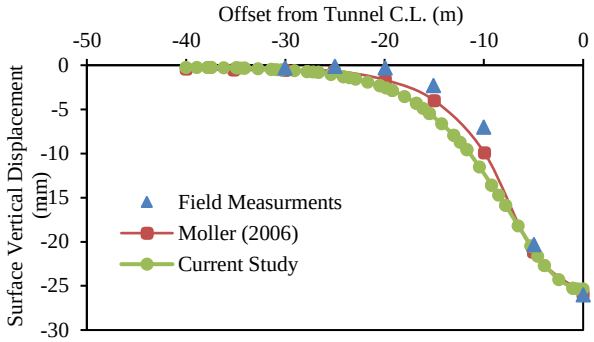

Figure 2. Greenfield surface settlement trough after the 3D model verification of the Second Heinenoord tunnel

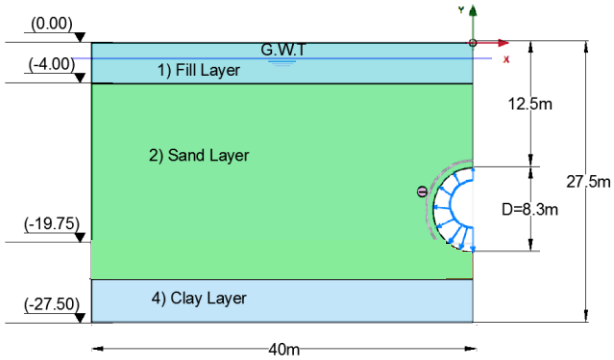

Figure 3. 2D model configuration of Second Heinenoord Tunnel after Moller (2006)

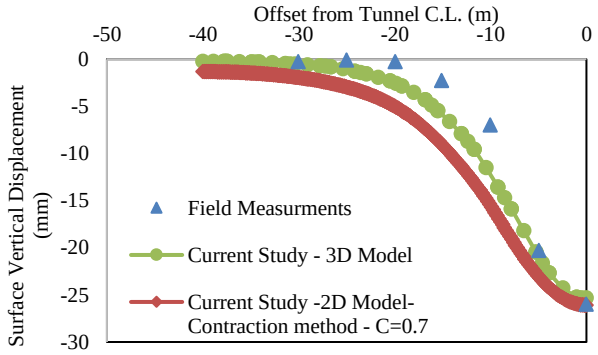

Figure 4. Greenfield surface settlement trough after the 2D model verification of the Second Heinenoord Tunnel

3 RAFT CONFIGURATION, GRANULAR MATERIALS PROPERTIES AND STAGES OF CONSTRUCTION

The effect of tunnel construction on a raft foundation is studied. The raft is characterized by the following; raft dimensions are 20 m width x 20 m length, the raft thickness is 1 m and the spacing between columns is 4.5 m. The columns loads have been selected such that the average stress beneath the raft foundation is 100 kPa. The raft is

simulated as a plate element with linear elastic concrete material properties such that the Young's Modulus of concrete = 7 x 10^7 kN/m^2 and Poisson's ratio u = 0.15. The proposed raft configuration is shown in Fig. 5.

In order to examine the effect of sand relative density on the tunnel-raft interaction, three different sandy soils are proposed (loose sand, medium dense sand and dense sand). The properties of these sandy soils are presented in Table 2.

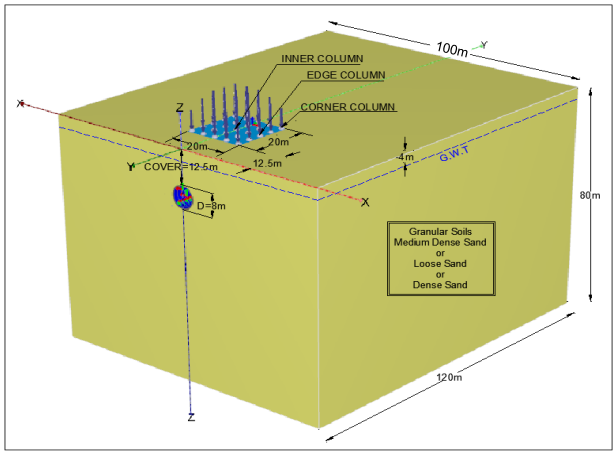

Figure 5. Proposed raft configuration and model boundaries

For the 3D analysis, the approach proposed by Moller (2006) has been adopted to account for the tunnel stages of construction. In the initial stage, initial stresses are generated using the at-rest lateral earth pressure procedure (K_o procedure) as indicated in Table 2. In the first stage, the raft and the column loads are activated. In the second stage, the five slices of the TBM shield and the face pressure are activated and the soil elements are deactivated at this segment. In the third stage, two slices of the grouting pressure are activated in addition to one slice of the hardening grout at the tail, the final lining is activated along these three slices at the tail and the gap is assigned for the two slices of the grouting pressure. In the fourth stage, as the tunnel advances, the TBM shield and face pressure are activated along the next segment and the soil element within this segment is deactivated. At the same stage, the shield on the previous segment is replaced by the lining element. The same procedure of the fourth stage is repeated until finishing the total tunnel length. It should be noted that the model boundaries shown in Fig 5. have been selected such that they have no effect on the raft settlement or the tunnel induced settlement.

For the 2D analysis, the contraction approach has been used. In the initial stage, initial stresses are generated using the at-rest lateral earth pressure procedure. In the first stage, the raft and the column loads are activated. In the second stage, the soil volume element inside the tunnel is deactivated and the tunnel lining and the rigid interface around the tunnel lining are activated. For the last stage, the contraction ratio (C) is applied around the tunnel lining.

Table 2. Proposed properties for sandy soils of different relative densities

Layer	Loose sand	Medium Dense Sand	Dense Sand
Unsaturated unit weight, γ_{unsat}(kN/m^3)	15	16	17
Saturated unit weight, γ_{sat} (kN/m^3)	17	18	19
Tangent stiffness for primary oedometer loading, E^{ref}_{oed} (MPa)	15	35	60
Secant stiffness in standard drained triaxial test, E^{ref}_{50} (MPa)	15	35	60
Unloading/Reloading stiffness, E^{ref}_{ur} (MPa)	45	105	180
Power for stress-level dependency of stiffness, m	0.5	0.5	0.5
Effective angle of shearing resistance, φ (deg.)	32	35	39
Effective cohesion, c' (kPa)	0.01	0.01	0.01
At rest Earth pressure coefficient, K_o	0.47	0.426	0.37
Poisson's ratio, υ_{ur}	0.3	0.25	0.2

4 3D SENSITIVITY ANALYSIS

The influence of tunnel diameter has been investigated in sandy soils. The selected tunnel diameters are between 4 m and 12 m with an increment of 2 m. Figure 6 shows that the tunnel diameter (D) has a great effect on the induced raft total and differential settlements. Figure 6 reveals that as the tunnel diameter increases, the raft total and differential settlements increase linearly. For medium dense sand, the initial settlement is 57 mm (case of no tunnel). This settlement increases to 66 mm when a 4 m tunnel diameter is excavated with an increasing percentage of 16%. For the largest tunnel diameter (D = 12 m), the raft total settlement increases by 68% (96 mm). Hence, increasing the tunnel diameter by a 2 m increment increases the raft settlement by about 4 mm.

In this study, the raft differential settlement is defined as the raft maximum settlement minus the raft minimum settlement. Figure 6 shows that the initial differential settlement is 5.5 mm (case of no tunnel). The raft differential settlement increase to 6.7 mm and 12 mm when 4 m tunnel and 12 m tunnel diameters are executed with increasing percentages of 20% and 70%, respectively. The observed trend could be attributed to the increased volume loss around the tunnel lining while increasing the tunnel diameter.

The effect of the tunnel cover is investigated at tunnel diameter = 8 m in medium dense sand formation. Different

values of the tunnel cover to diameter (Z/D) ratio ranging between 0.5 and 4.0 have been investigated. Figure 7. depicts the influence of changing the tunnel cover to diameter ratio (Z/D) on the raft total and differential settlements and relate them to the initial case before the tunnel construction. Figure 7 reveals that as the tunnel cover to diameter ratio (Z/D) increases, the raft total and differential settlements decrease. Consequently, the influence of tunnelling process on raft diminishes as the tunnel cover increases. The effect of tunnelling process on the raft induced differential settlement vanishes at Z/D = 2.5. This trend could be attributed to the tunnel influence zones. As the tunnel gets deeper, it affects larger surface area hence the changes in the induced surface settlement within the raft area is limited, that is why the raft differential settlement decreases.

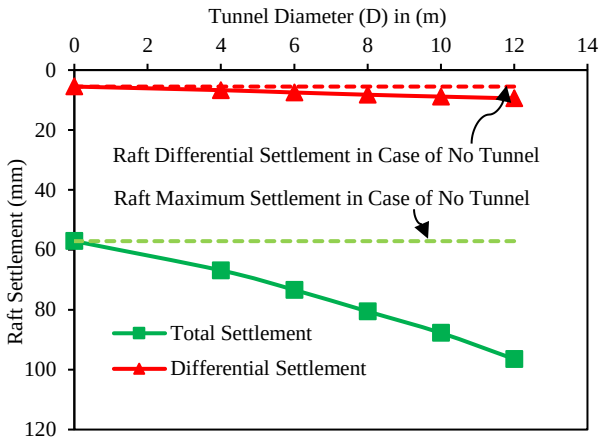

Figure 6. Influence of tunnel diameter (D) on raft performance for the case of medium dense sand

Figure 8. presents the effect of changing the horizontal clearance (CL) between the tunnel centerline and the raft centerline on the raft performance. Figure 8 shows that the effect of the tunnel construction on the existing raft foundations vanishes at CL = 30 m. In addition, the maximum value of raft total settlement is observed when the tunnel centerline is at the mid distance between the raft centerline and the raft edge (i.e. CL = 5 m). Moreover, the maximum value of raft differential settlement is noted when the tunnel centerline is directly beneath the raft edge (i.e. CL = 10 m). While increasing the horizontal clearance, the raft moves away from the tunnel influence zone and this explains the decreasing effect of the tunnel construction process on the raft foundation when the horizontal clearance decreases.

5 2D CONTRACTION RATIO (C)

Based on the previous 3D sensitivity analysis, a complete database for raft settlement trough due to the tunnelling process is achieved considering the effect of soil relative density, tunnel diameter (D), tunnel cover (Z), and the horizontal clearance (CL). Afterwards, a series of 2D trials have been conducted by testing different contraction ratio values (C) in order to acquire the same settlement troughs for the raft foundation obtained from 3D models.

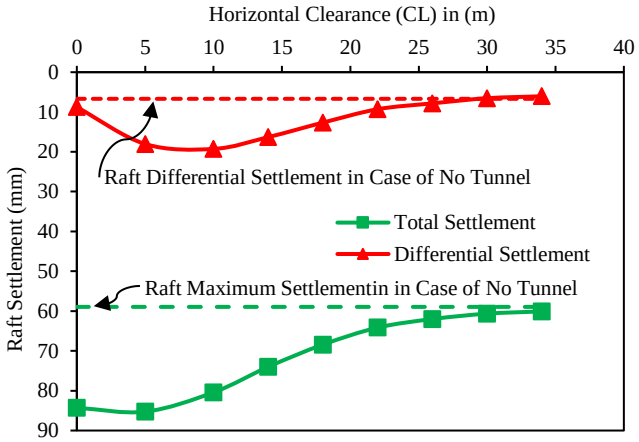

Figure 7. Influence of tunnel cover to diameter ratio (Z/D) on raft performance for the case of medium dense sand

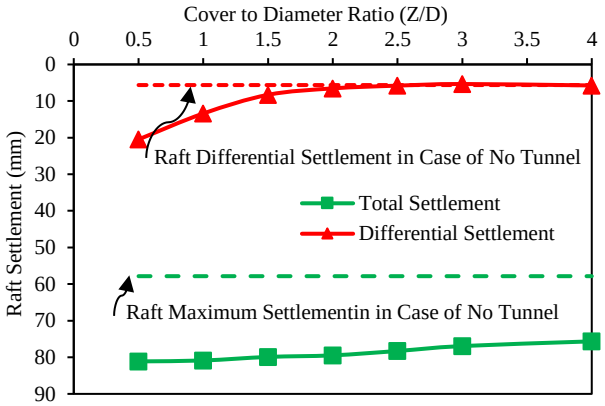

Figure 8. Influence of horizontal clearance (CL) on raft performance for the case of medium dense sand

.

Figures 9 and 10 depict the adopted contraction ratio values (C) for different tunnel diameters (D) and different tunnel covers to diameter ratios (Z/D). For loose sand, the contraction ratio (C) ranges between 1.3 and 1.1 with an average value of 1.2. Whereas, for medium dense sand, it ranges between 0.54 and 0.47 with an average value of 0.5. For the dense sand, it ranges between 0.28 and 0.24 with an average value of 0.26. The value of the contraction ratio is found to depend mainly on the soil relative density, whilst, the tunnel diameter (D) and Z/D have a slight effect.

Figure 11 shows that contraction ratio (C) is greatly affected by the horizontal clearance between the tunnel centerline and the raft centerline (CL) especially in loose sand formation. For loose sand, the contraction ratio ranges between 0.8 and 1.3 with an average value of 1.0. For medium dense and dense sands there is a slight change in the adopted contraction ratio while changing CL.

The average values of contraction ratio (C) for the case of medium dense and dense sands are observed to be 0.5 and 0.25 respectively.

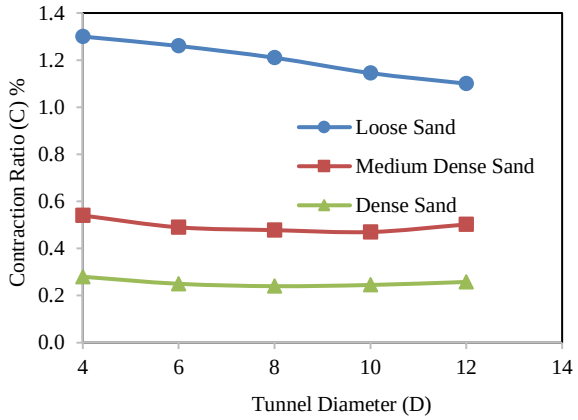

Figure 9. Adopted contraction ratio (C) when changing the tunnel diameter (D) for (Z/D) = 1.5

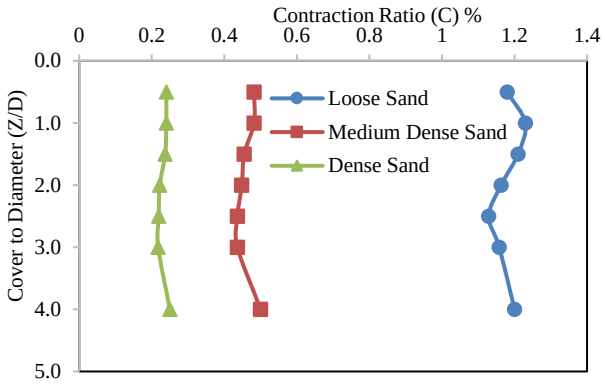

Figure 10. Adopted contraction ratio (C) when changing the tunnel cover to diameter ratio (Z/D) for D = 8 m

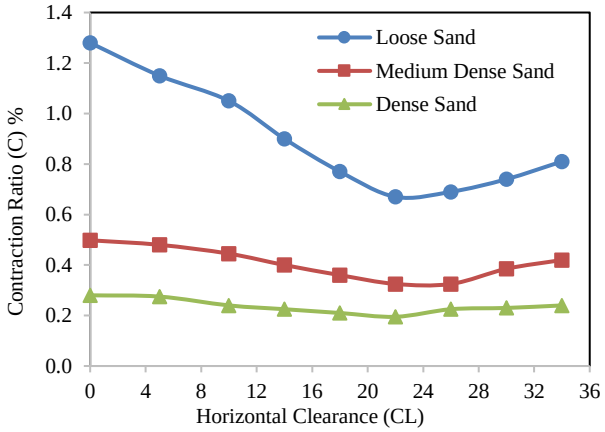

Figure 11. Adopted contraction ratio (C) when changing the horizontal clearance (CL) for (Z/D) = 1.5

6 CONCLUSIONS

In this study, the numerical simulation of the tunnel construction process is achieved in both 2D and 3D using the finite element software PLAXIS ©. The numerical simulations have been validated by comparing the results of the numerical analyses with the field measurements of the greenfield surface settlement trough monitored during the construction of the Second Heinenoord tunnel in the Netherlands. The validation of the numerical analysis helped in studying the effect of the tunnel construction process on an existing raft foundation while considering different geometrical configurations between the raft and the tunnel in sandy soils.

A sensitivity analysis has been conducted using the 3D finite element models to investigate the performance of an existing raft foundation under the effect of related parameters, such as: soil relative density (D_r), tunnel diameter (D), tunnel cover (Z) and horizontal clearance between tunnel centerline and raft centerline (CL). Increasing the tunnel diameter increases the raft total settlement and differential settlement. The differential settlement is increased from 5.5 mm where there is no tunnel to 6.7 mm when excavating a 4 m tunnel diameter and 12 mm when excavating a 12 m tunnel diameter. This could be attributed to the volume loss rising as the tunnel diameter increases. It is also noted that, increasing the tunnel cover to diameter ratio (Z/D) decreases the raft maximum total and differential settlements. The induced raft differential settlement due to the tunnelling process vanishes at (Z/D) equals 2.5. This could be attributed to the tunnel influence zones. For cover to diameter ratio (Z/D) larger than 2.5, the raft foundation is located inside the same zone of the induced settlement due to the tunnelling process. In addition, this study reveals that the effect of the tunnelling process vanishes at horizontal clearance (CL) between the tunnel centerline and the raft centerline equals 30 m. Moreover, the maximum differential settlement occurs when the tunnel centerline is located just beneath the raft edge.

The results of the 3D model have been used to predict the values of the contraction ratio that should be used in the 2D analysis to account for the 3D arching effect and volume loss. This has been achieved by examining different contraction ratio values such that the 2D model provides a raft settlement trough similar to the one resulted from the 3D model. The contraction ratio has been investigated for different relative densities (loose, medium dense and dense sands) while changing the tunnel related parameters (tunnel diameter (D), tunnel cover (Z) and horizontal clearance (CL) between tunnel centerline and raft centerline). This study reveals that, the contraction ratio is mainly affected by the sand relative density and horizontal clearance between tunnel centerline and raft centerline (CL), whilst, the tunnel diameter and the tunnel cover to diameter ratio (Z/D) have insignificant effect. In the preliminary stages of projects that involve studying the effect of the tunnelling process on an existing raft foundation, average values of contraction ratio (C) of 1.0, 0.5, and 0.25 may be adopted for loose, medium dense and dense sand, respectively.

7 REFERENCES

Addenbrooke, T.I., and Potts, D.M. 1997. A structure's influence on tunnelling-induced ground movements. *ICE Journal of Geotechnical Engineering*, 125(02): 109-125.

Franzuis, J. N. 2003. Behavior of Building due to tunnel induced subsidence. Ph.D. Dissertation, Department of Civil and Environmental Engineering, Imperial College of Science, Technology and Medicine, London.

Maleki, M.H., Sereshteh, M., Mousivand, M., and Bayat. 2011. An equivalent beam model for the analysis of tunnel-building interaction. *Tunnel Underground Space Technology,* 26(4):524-533.

Moller, S. 2006. Tunnel induced settlements and structural forces in lining. Ph.D. Dissertation, Department of Geotechnical Engineering, University of Stuttgart, Stuttgart.

Mroueh, H., and Shahrour, I. 2003. A full 3-D finite element analysis of tunnelling–adjacent structures interaction. *Computers and Geotechnics,* 30:245–253.

O'Reilly, M.P., and New, B.M. 1982. Settlements above tunnels in the United Kingdom: their magnitude and prediction. *Tunnelling, 82:173–181.*

Peck, R.B. 1969. Deep excavation and tunnelling in soft ground. *In* Proceedings of 7th International Conference on Soil mechanic Foundation Engineering, Mexico, pp. 225–290.

Sugiyama, T., Hagiwara, T., Nomoto, T., Nomoto, M., Ano, Y., Mair, R.J., Bolton, M.D., and Soga, K. 1999. Observations of ground movements during tunnel construction by slurry shield method at the Docklands Light Railway Lewisham extension – East London. *Soils and Foundations,* 39(3): 99–112.

Vermeer, P.A., and Brinkgreve R.B.J. 2001. PLAXIS finite element code for soil and rock analyses.

Wood, A.M. 1975. The circular tunnel in elastic ground. Geotechnique, 25(1):115–127.